Inorganic Chemistry

Article

pubs.acs.org/IC

Synthesis of Bis(imidazole) Metal Complexes and Their Use in Rapid NO Detection and Quantification Devices

Eric Victor, Sunghee Kim, and Stephen J. Lippard*

Department of Chemistry, Massachusetts Institute of Technology, Cambridge, Massachusetts 02139, United States

Supporting Information

ABSTRACT: To explore the release of nitrogen oxide gases from reaction solutions, we developed a series of colorimetric sensors based on the *cis*-nitrogen-donating ligand bis(1-methylimidazol-2-yl)phenylmethoxymethane (BIPhMe). The complexes M(BIPhMe)X_2, where M is Fe^{2+} or Co^{2+} and X is Cl^-, Br^-, or I^-, were prepared and structurally and spectroscopically characterized. The reactivity of these complexes toward NO(g) and NO_2(g) in solution was explored. These complexes were then incorporated into test strips and syringes to provide devices that can qualitatively, and in the case of the syringes quantitatively, detect NO(g) and NO_2(g) in a reaction headspace without additional equipment.

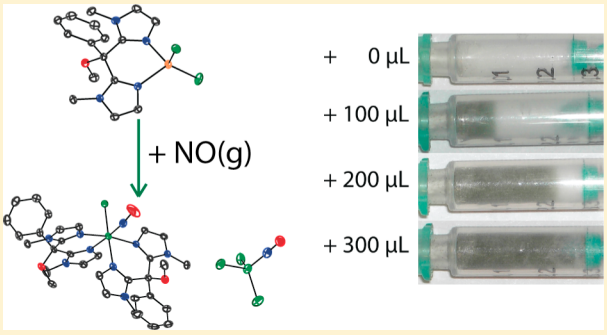

INTRODUCTION

The discovery of nitric oxide (NO) as a biological signaling agent has resulted in an increased interest in the study of the molecule.[1] Researchers in fields ranging from synthetic inorganic chemistry to molecular biology investigate the properties, reactivity, and impact of NO on living systems.[2] It is often desirable to observe and quantify the release of NO(g) or NO_2(g) from a reaction in biology and chemistry, and there are many methods to do so. There currently exist multiple methods to perform these experiments.[3] The detection of NO(g) can be achieved by reaction with O_3(g) and measurement of the subsequent chemiluminescence.[4] Electrochemical methods oxidize NO$^\bullet$ to NO^+ and monitor the change in amperage using a Clark-like electrode.[5] These approaches can provide solution concentrations of NO$^\bullet$ but cannot measure the release of NO(g) to the surrounding headspace and require an additional instrument that may not be commonly available or can alter the observed reaction. Small molecules have also been employed as reaction-based methods for detection and quantification.

Iron(II) porphyrin compounds have been used to detect and quantify the release of NO(g) by IR, UV−vis, and electron paramagnetic resonance spectroscopy following their capture as [Fe^{II}(porphyrin)(NO)].[6] These methods provide a rapid means to detect the release of NO(g) using instruments available in most chemistry laboratories but, owing to the strong intensity of the porphyrin absorbance bands, do not provide a facile method for observing NO liberation by the naked eye.

Commercial NO colorimetric detection kits are available that indirectly measure NO by converting it to a higher NO_x species and subsequently quantifying the concentration of nitrate and nitrite present in solution using the Griess reagent.[7] This method can result in incorrect measurements owing to NO_2^- contamination or loss of NO(g) to the surrounding headspace.

The complexes $[Cu(dmp)_2]^{2+}$ and $[Cu(RB{-}Py)]^{2+}$, and a tetraarylcalix[4]arene ether radical (Chart 1), exhibit colorimetric responses upon NO$^\bullet$ exposure.[8] The mechanism of response of the Cu^{2+} complexes involves reduction to Cu^+, resulting in changes from pale green to bright yellow/orange and from colorless to pink, respectively, for the two compounds noted. This response mechanism is similar to that of the NO fluorescent probe CuFL1.[9] The tetraarylcalix[4]arene radical binds NO$^\bullet$, eliciting a color change from bright green to dark

Chart 1. Colorimetric and Fluorescent Probes To Detect NO$^\bullet$

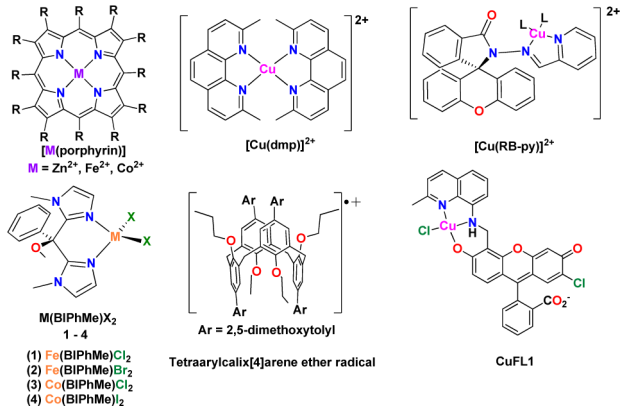

Received: July 22, 2014
Published: November 24, 2014

   dx.doi.org/10.1021/ic501765g | *Inorg. Chem.* 2014, 53, 12809−12821

blue. An excellent review article detailing the analytical techniques currently available to detect NO is available.[3]

In the present work, we devised a set of colorimetric sensors using Fe^{2+} and Co^{2+} halide complexes of bis(1-methylimidazol-2-yl)phenylmethoxymethane (BIPhMe), which contains two *N*-donor atoms.[10] The NO(g) and NO_2(g) chemistry of these complexes was explored, and the products were characterized by X-ray crystallography, electrospray ionization mass spectrometry (ESI-MS), and Mössbauer, IR, UV−vis, and ^{1}H NMR spectroscopy. We utilized these compounds in colorimetric test strips and headspace analyzers capable of providing simple and rapid methods to observe the release of NO(g) and NO_2(g) from chemical and biological reactions. The results of these studies constitute the present report.

EXPERIMENTAL SECTION

General Procedures. All manipulations were performed under an atmosphere of nitrogen gas using standard Schlenk techniques or in an MBraun glovebox under an atmosphere of purified nitrogen. Nitric oxide (NO; Airgas, 99%) was purified by a literature procedure.[11] The NO(g) stream was passed through an Ascarite column (NaOH fused on silica gel) and a 6 ft. coil filled with silica gel that was cooled to −78 °C using a dry ice/acetone bath. NO was stored using standard gas bulbs. Nitrogen dioxide (NO_2; Sigma-Aldrich, ≥99.5%) was purified by condensation in a standard gas bulb at −78 °C followed by vacuum distillation to remove higher-boiling impurities. Carbon monoxide (CO; Sigma-Aldrich, 99%) and hydrogen sulfide (H_2S; Sigma-Aldrich, 99.5%) were used as received and stored in 50 mL Schlenk flasks. All stored gases were transferred using Hamilton gastight syringes equipped with a three-way valve and a needle outlet. A dioxygen (O_2; Airgas, 99%) gas stream was passed through a Drierite column prior to use. Water (H_2O) was purified in a Milli-Q water filtration system to a resistance of 18 mΩ/cm and deoxygenated with nitrogen gas for 2 h prior to transfer by a Hamilton gastight syringe. Diethyl ether (Et_2O), pentane, methylene chloride, tetrahydrofuran (THF), and acetonitrile (MeCN) were purified using a Glass Contour solvent system.[12] Deuterated solvents were purchased from Cambridge Isotope Laboratories Inc. (Tewksbury, MA). BIPhMe was synthesized according to a literature procedure.[10] All organic chemicals were purchased from Sigma-Aldrich and used as received. Metal salts were purchased from Strem Chemicals and used as received.

Physical Measurements. NMR spectra were recorded on a Bruker Avance spectrometer operating at 400 MHz at ambient temperature and referenced to residual signals in the deuterated solvent. Matrix-assisted laser desorption ionization time-of-flight mass spectrometry (MALDI-TOF-MS) spectra were obtained with a Bruker Omniflex MALDI-TOF-MS spectrometer with a Reflectron accessory. Low-resolution ESI-MS spectra were obtained with an Agilent 1100 series LC/MSD mass spectrometer using degassed MeCN as the carrier solvent. Extinction coefficients were determined using a Cary 50 UV−vis spectrometer. Fourier transform infrared (FT-IR) spectra were recorded on a Thermo Nicolet Avatar 360 spectrometer running the *OMNIC* software package; solid samples were pressed into KBr disks, and solution samples were prepared in an airtight Graseby-Specac solution cell with CaF_2 windows and 0.1 mm spacers. Samples for ^{57}Fe Mössbauer studies were prepared by grinding a solid sample with Apiezon-N grease. These ^{57}Fe Mössbauer samples were placed in an 80 K cryostat during measurement. A ^{57}Co/Rh source was moved at a constant acceleration at room temperature against the absorber sample. All isomer shift (δ) and quadrupole splitting (ΔE_Q) values are reported with respect to the ^{57}Fe-enriched metallic iron foil that was used for velocity calibration. The displayed spectrum was folded to enhance the signal-to-noise ratio. Fits of the data were calculated by the *WMOSS* plot-and-fit program, version 2.5.[13]

X-ray Data Collection, Structure, and Solution Refinement. Crystals of **1**−**9** suitable for X-ray diffraction were mounted in Paratone N oil and frozen under a nitrogen cold stream maintained at 100 K by a KRYO-FLEX low-temperature apparatus. Data were collected on a Bruker APEX CCD X-ray diffractometer with Mo Kα radiation (λ = 0.71073 Å) controlled by the *APEX2* software package.[14] Empirical absorption corrections were calculated with *SADABS*.[15] The structures were solved by direct methods with refinement by full-matrix least squares based on F^2 using *SHELXTL-97*.[16] All non-hydrogen atoms were located and refined anisotropically. Hydrogen atoms were assigned to idealized positions and given thermal parameters equal to either 1.5 (methyl hydrogen atoms) or 1.2 (nonmethyl hydrogen atoms) times the thermal parameters of the atoms to which they were attached. Figures were generated using the *Olex2.1* Graphical User Interface.[17] See Tables 2 and 4 for crystallographic data and refinement details.

[Fe(BIPhMe)Cl$_2$], 1. A 50 mL Erlenmeyer flask was charged with $FeCl_2{\cdot}4H_2O$ (227.5 mg, 1.144 mmol) and BIPhMe (336.0 mg, 1.190 mmol). THF (20 mL) was added to the flask, and the reacting solution was stirred for 1 h, during which time a white precipitate formed. The precipitate was filtered, and the solid was washed with THF (3 × 10 mL) and Et_2O (3 × 20 mL) and then dried in vacuo. The yield was 417.6 mg (1.021 mmol, 74%) of **1**. X-ray-quality crystals were grown by vapor diffusion of Et_2O into a methylene chloride solution of **1**. Anal. Calcd for $C_{16}H_{18}Cl_2FeN_4O$: C, 46.98; H, 4.43; N, 13.70. Found: C, 47.12; H, 4.45; N, 13.51. MALDI-TOF-MS (anthracene, *m*/*z*): 408.17 (calcd $[M]^+$: 408.02), 373.12 (calcd $[M - Cl]^+$: 373.05). ESI-MS (MeCN, *m*/*z*): 373.1 (calcd $[M - Cl]^+$: 373.1), 655.2 (calcd [M + BIPhMe − Cl]$^+$: 655.2). ^{1}H NMR (400 MHz, $CDCl_3$, ppm): 1.88 (s), 3.77 (s), 9.42 (s), 10.93 (s), 18.82 (s), 21.90 (br), 29.15 (s), 37.27 (s). FT-IR (KBr, cm^{-1}): 3156 (w), 3139 (w), 3118 (m), 3067 (w), 3009 (w), 2954 (m), 2834 (m), 1630 (w), 1603 (w), 1541 (m), 1500 (s), 1470 (m), 1449 (s), 1400 (m), 1350 (w), 1323 (m), 1284 (s), 1225 (w), 1212 (w), 1174 (m), 1174 (s), 1146 (s), 1090 (sh), 1071 (s), 1032 (w), 990 (s), 940 (w), 898 (s), 760 (s), 733 (s), 703 (s), 688 (w), 645 (m), 558 (w), 512 (w), 465 (w). ^{57}Fe Mössbauer (mm/s; 80 K, δ mm/s, ΔE_Q mm/s, Γ mm/s): 0.929(2), 3.127(2), 0.354(2).

[Fe(BIPhMe)Br$_2$], 2. In a 20 mL vial, $FeBr_2$ (330.2 mg, 1.531 mmol) was dissolved in THF (10 mL), and a solution of BIPhMe (422.0 mg, 1.495 mmol) in THF (10 mL) was added dropwise over 1 min. The solution was stirred for 1 h, during which time a pale-brown precipitate formed and was collected on an F-grade frit. The precipitate was washed with THF (3 × 10 mL) and Et_2O (3 × 20 mL), dried in vacuo, and collected to yield 569.1 mg (1.143 mmol, 77%) of **2**. X-ray-quality crystals were grown by vapor diffusion of Et_2O into a methylene chloride solution of **2**. Anal. Calcd for $C_{16}H_{18}Br_2FeN_4O$: C, 38.59; H, 3.64; N, 11.25. Found: C, 38.39; H, 3.34; N, 11.06. ESI-MS (MeCN, *m*/*z*): 417.0 (calcd $[M - Br]^+$: 417.0), 699.2 (calcd [M + BIPhMe − Br]$^+$: 699.1). ^{1}H NMR (400 MHz, $CDCl_3$, ppm): 2.82 (br), 9.72 (s), 11.03 (s), 23.09 (br), 23.36 (s), 33.59 (s), 38.54 (s). FT-IR (KBr, cm^{-1}): 3153 (w), 3143 (w), 3120 (m), 3056 (w), 3005 (w), 2954 (w), 2833 (w), 1709 (w), 1691 (w), 1603 (m), 1542 (m), 1498 (s), 1468 (m), 1448 (s), 1398 (w), 1349 (w), 1322 (w), 1284 (s), 1225 (w), 1212 (w), 1174 (m), 1145 (m), 1089 (m), 1070 (s), 988 (s), 939 (w), 898 (s), 759 (s), 723 (s), 702 (s), 645 (m), 627 (w), 556 (w), 511 (w), 465 (w). ^{57}Fe Mössbauer (mm/s; 80 K, δ mm/s, ΔE_Q mm/s, Γ mm/s): 0.901(2), 3.322(2), 0.255(2).

[Co(BIPhMe)Cl$_2$], 3. To a 20 mL vial was added anhydrous $CoCl_2$ (212.0 mg, 1.633 mmol) and BIPhMe (460.0 mg, 1.629 mmol). The solids were dissolved in a mixture of THF (12 mL) and methylene chloride (4 mL). The solution was stirred for 1 h, resulting in a deep-blue precipitate. The precipitate was collected by filtration, washed with THF (2 × 5 mL) and Et_2O (3 × 20 mL), and dried in vacuo to afford 619.6 mg (1.503 mmol, 92%) of **3**. X-ray-quality crystals of **3** were grown by vapor diffusion of Et_2O into an MeCN solution. Anal. Calcd for $C_{16}H_{18}Cl_2CoN_4O$: C, 46.62; H, 4.40; N, 13.59. Found: C, 46.28; H, 4.15; N, 13.39. ESI-MS (MeCN, *m*/*z*): 376.1 (calcd $[M - Cl]^+$: 376.1), 658.3 (calcd [M + BIPhMe − Cl]$^+$: 658.2). ^{1}H NMR (400 MHz, $CDCl_3$, ppm): 9.12 (s, 1H), 10.56 (s, 2H), 13.08 (s, 3H), 17.75 (s, 6H), 19.70 (br, 1H), 33.78 (s, 2H), 37.93 (br, 2H). FT-IR (KBr, cm^{-1}): 3143 (w), 3116 (m), 3056 (w), 2999 (w), 2956 (m), 2928 (w), 2889 (w), 2823 (w), 1679 (w), 1594 (w), 1533 (w), 1493 (s), 1461 (m), 1446 (s), 1393 (w), 1348 (w), 1317 (w), 1283 (s),

dx.doi.org/10.1021/ic501765g | *Inorg. Chem.* 2014, 53, 12809−12821

1222 (m), 1207 (w), 1182 (m), 1168 (m), 1142 (m), 1085 (s), 1066 (s), 1031 (w), 985 (s), 949 (w), 932 (w), 891 (s), 841 (w), 755 (s), 719 (s), 702 (s), 642 (m), 554 (w), 508 (w), 461 (w). UV−vis [MeCN; λ, nm (ε, M^{-1} cm^{-1})]: 531 (155 ± 4), 555 (259 ± 5), 611 (422 ± 5), 631 (490 ± 4).

[Co(BIPhMe)I_2], 4. To a 50 mL Erlenmeyer flask was added anhydrous CoI_2 (325.5 mg, 1.041 mmol) and BIPhMe (306.6 mg, 1.083 mmol). The solids were dissolved in a mixture of THF (20 mL) and methylene chloride (2 mL). The solution was stirred for 1 h, resulting in a green solution. Pentanes (30 mL) were added to precipitate the product as a green microcrystalline solid. The precipitate was filtered, washed with pentanes (3 × 10 mL), and dried under vacuum for 5 h, affording 579.8 mg (0.973 mmol, 93%) of **4**. X-ray-quality crystals of **4** were grown by vapor diffusion of Et_2O into a methylene chloride solution. Anal. Calcd for $C_{16}H_{18}I_2CoN_4O$: C, 32.29; H, 3.05; N, 9.41. Found: C, 31.98; H, 2.81; N, 9.32. ESI-MS (MeCN, m/z): 750.2 (calcd [M + BIPhMe − I]$^+$: 750.1), 468.0 (calcd [M − I]$^+$: 468.0), 579.6 (calcd [M − CH_3]$^-$: 579.9), 126.8 (calcd [I]$^-$: 126.9). ^{1}H NMR (400 MHz, $CDCl_3$, ppm): 9.60 (s, 1H), 11.20 (s, 2H), 17.01 (s, 2H), 22.30 (s, 6H), 28.13 (br, 1H), 34.64 (s, 2H). FT-IR (KBr, cm^{-1}): 3162 (w), 3130 (m), 3079 (w), 2973 (w), 2928 (w), 2898 (w), 2863 (w), 2829 (w), 1649 (w), 1550 (w), 1505 (s), 1449 (m), 1408 (w), 1355 (w), 1285 (s), 1224 (m), 1150 (s), 1090 (m), 1072 (m), 1031 (s), 992 (m), 938 (w), 900 (m), 762 (s), 725 (s), 704 (m), 637 (s), 572 (m), 517 (m), 472 (w). UV−vis [MeCN; λ, nm (ε, M^{-1} cm^{-1})]: 310 (2123 ± 105), 373 (1506 ± 69), 583 (289 ± 16), 607 (424 ± 21), 639 (596 ± 28), 668 (449 ± 22).

[Fe(BIPhMe)$_2$(NO)Cl][Fe(NO)Cl_3], 5. In a 20 mL vial, **1** (58.2 mg, 0.143 mmol) was dissolved in methylene chloride (2 mL). The reaction vessel was capped with a rubber septum, and NO(g) (7.5 mL, 0.30 mmol) was injected under vigorous stirring. The solution instantly turned from colorless to dark green. The solution was stirred for an additional 1 h and filtered through glass microfiber filter paper. X-ray-quality crystals of the product were formed upon vapor diffusion of Et_2O over the course of 2 days. These dark-green crystals were collected by filtration and washed with Et_2O (3 × 5 mL), resulting in a yield of 41.6 mg (47.4 μmol, 33%) of **5**. Anal. Calcd for $C_{32}H_{36}Cl_4Fe_2N_{10}O_4$: C, 43.77; H, 4.13; N, 15.95. Found: C, 43.42; H, 4.34; N, 16.13. ESI-MS (MeCN, m/z): 655.2 ([CAT − NO]$^+$, calcd 655.2), 125.8 ([AN − NOCl]$^-$, calcd 125.9), 160.6 ([AN − NO]$^-$, calcd 160.8). FT-IR (KBr, cm^{-1}): 3121 (m), 3054 (w), 2958 (m), 2928 (m), 2829 (w), 1792 (ν_{NO}), 1709 (ν_{NO}), 1656 (s), 1606 (w), 1542 (w), 1498 (s), 1468 (w), 1448 (m), 1400 (w), 1351 (w), 1322 (w), 1282 (s), 1226 (w), 1171 (m), 1143 (m), 1089 (m), 1072 (s), 1032 (w), 988 (s), 935 (w), 898 (s), 761 (s), 723 (s), 702 (s), 644 (m), 510 (w), 466 (w). UV−vis [MeCN; λ, nm (ε, M^{-1} cm^{-1})]: 363 (850 ± 40), 473 (340 ± 30), 699 (220 ± 10).

[Fe(BIPhMe)$_2$(NO)Br][Fe(NO)Br_3], 6. In a 20 mL vial, **2** (20.4 mg, 0.0371 mmol) was dissolved in methylene chloride (2 mL). The reaction vessel was capped with a rubber septum, and NO(g) (3.7 mL, 0.15 mmol) was injected under vigorous stirring. The solution instantly turned from colorless to dark red. The solution was stirred for an additional 1 h and filtered through a piece of glass microfiber filter paper. Dark-red crystals were grown by vapor diffusion of Et_2O into a methylene chloride solution, collected by filtration, and washed with Et_2O (3 × 5 mL), resulting in a yield of 7.2 mg (6.8 μmol, 18%) of **6**. Anal. Calcd for $C_{32}H_{36}Br_4Fe_2N_{10}O_4$: C, 36.40; H, 3.44; N, 13.26. Found: C, 36.55; H, 3.57; N, 13.33. ESI-MS (MeCN, m/z): 701.1 ([Cat − NO]$^+$, calcd 701.2), 213.6 ([An − NOBr]$^-$, calcd 213.8), 296.5 ([An − NO]$^-$, calcd 296.7). FT-IR (KBr, cm^{-1}): 3120 (m), 3061 (w), 3006 (w), 2955 (m), 2928 (m), 2829 (m), 1791 (ν_{NO}), 1705 (ν_{NO}), 1656 (m), 1597 (w), 1542 (w), 1497 (s), 1468 (m), 1448 (m), 1399 (w), 1350 (w), 1322 (w), 1282 (s), 1226 (w), 1208 (w), 1171 (m), 1143 (m), 1089 (m), 1071 (s), 1032 (w), 988 (s), 935 (w), 897 (s), 761 (s), 723 (s), 702 (m), 645 (m), 557 (w), 510 (w), 466 (w). UV−vis [MeCN; λ, nm (ε, M^{-1} cm^{-1})]: 370 (2780 ± 200), 490 (750 ± 30), 701 (360 ± 20).

Synthesis of [Fe(BIPhMe)$(NO_3)_2$Cl], 7. In a 20 mL vial, **1** (20.0 mg, 0.0489 mmol) was dissolved in methylene chloride (2 mL). The reaction vessel was capped with a rubber septum, and NO_2(g) (3.7 mL, 0.15 mmol) was injected under vigorous stirring. The solution instantly turned from colorless to yellow. The solution was stirred for an additional 1 h and filtered through a piece of glass filter paper in a Pasteur pipet. X-ray-quality crystals of the product were formed upon vapor diffusion of Et_2O over the course of 2 days. The crystals were collected by filtration and washed with Et_2O (3 × 5 mL), resulting in a yield of 9.7 mg (0.018 mmol, 37%) of **7**. Anal. Calcd for $C_{16}H_{18}ClFeN_6O_7$: C, 35.45; H, 3.35; N, 15.50. Found: C, 35.55; H, 3.59; N, 15.33. ESI-MS (MeCN, m/z): 682.2 (calcd [M + BIPhMe − NO_3 − Cl]$^+$: 682.2), 655.2 (calcd [M + BIPhMe − 2NO_3]$^+$: 655.2). FT-IR (KBr, cm^{-1}): 3120 (m), 3058 (w), 2997 (w), 2954 (m), 2931 (m), 2824 (w), 1653 (w), 1546 (w), 1493 (s), 1467 (s), 1448 (m), 1384 (m), 1352 (m), 1282 (w), 1227 (w), 1208 (m), 1169 (w), 1153 (w), 1132 (m), 1090 (m), 1073 (m), 1032 (w), 987 (m), 949 (w), 936 (w), 900 (s), 846 (m), 761 (s), 722 (s), 702 (s), 644 (w), 556 (w), 511 (w). UV−vis [MeCN; λ, nm (ε, M^{-1} cm^{-1})]: 335 (570 ± 40).

Synthesis of [Fe(BIPhMe)$(NO_3)_2$Br], 8. In a 20 mL vial, **2** (20.0 mg, 0.0489 mmol) was dissolved in methylene chloride (2 mL). The reaction vessel was capped with a rubber septum, and NO_2(g) (3.7 mL, 0.15 mmol) was injected under vigorous stirring. The solution instantly turned from colorless to yellow. The solution was stirred for an additional 1 h and filtered through a piece of glass filter paper in a Pasteur pipet. The crystals were collected by filtration and washed with Et_2O (3 × 5 mL), resulting in a yield of 9.7 mg (0.018 mmol, 37%) of **8**. Anal. Calcd for $C_{16}H_{18}BrFeN_6O_7$: C, 35.45; H, 3.35; N, 15.50. Found: C, 35.55; H, 3.59; N, 15.33. ESI-MS (MeCN, m/z): 701.1 (calcd [M + BIPhMe − 2NO_3]$^+$: 701.1), 682.1 (calcd [M + BIPhMe − NO_3 − Br]$^+$: 682.2). FT-IR (KBr, cm^{-1}): 3129 (m), 3062 (w), 2997 (w), 2954 (m), 2929 (m), 2829 (w), 1635 (w), 1545 (w), 1495 (s), 1468 (m), 1448 (m), 1384 (s), 1353 (s), 1282 (s), 1169 (m), 1154 (m), 1134 (m), 1090 (m), 1072 (s), 1032(w), 897 (m), 932 (w), 899 (s), 834 (m), 760 (s), 721 (s), 702 (m), 634 (w), 555 (w), 511 (w). UV−vis [MeCN; λ, nm (ε, M^{-1} cm^{-1})]: 290 (5800 ± 300), 360 (3500 ± 220).

Reaction of 3 with NO_2(g). In a 20 mL vial, **3** (27.7 mg, 0.0672 mmol) was dissolved in methylene chloride (2 mL). The reaction vessel was capped with a rubber septum, and NO_2(g) was injected until no further color change was observed. The solution turned from deep blue to dark green. The solution was stirred for 1 h and subsequently filtered through glass microfiber filter paper. The product was precipitated by addition of Et_2O (10 mL), collected by filtration, and dried under vacuum. The final product was a dark-green solid, and the collected yield was 17 mg. The exact structure of the product is currently unknown. ESI-MS (m/z): 660.7 (calcd [Co(BIPhMe)$_2H_2$Cl]$^+$: 660.2); 685.4 (calcd [Co(BIPhMe)$_2(NO_3)_2$]$^+$: 685.2); 780.3 (calcd [Co_2(BIPhMe)(NO_3)HCl]$^+$: 780.1). FT-IR (KBr, cm^{-1}): 3122 (m), 3058 (w), 2997 (w), 2935 (m), 2830 (w), 1652 (w), 1501 (s), 1471 (m), 1448 (s), 1385 (m), 1314 (s), 1286 (s), 1169 (s), 1149 (s), 1090 (m), 1072 (s), 1033 (w), 992 (s), 960 (w), 899 (s), 819 (m), 760 (s), 721 (s), 703 (s), 644 (m), 556 (w), 510 (w).

Reaction of 4 with NO(g). In a 20 mL vial, **4** (44.5 mg, 0.0748 mmol) was dissolved in THF (2 mL). The reaction vessel was capped with a rubber septum, and NO(g) was injected until no further color change was observed. The solution turned from emerald green to dark green. The solution was stirred for 1 h and subsequently filtered through glass microfiber filter paper. The product was precipitated by addition of Et_2O (10 mL), collected by filtration, and dried under vacuum. The final product was a dark-green solid, and the collected yield was 38 mg. The exact structural nature of the product is currently unknown. ESI-MS (m/z): 668.2 (calcd [Co(BIPhMe)$_2(NO)_2$]$^+$: 668.2); 371.1 (calcd [Co(BIPhMe)(NO)]$^+$: 371.1); 341.1 (calcd [Co(BIPhMe)]$^+$: 341.1); 439.6 (calcd [CoI_3]$^-$: 439.6); 380.5 (calcd [I_3]$^-$: 380.7); 312.6 (calcd [CoI_2]$^-$: 312.7). FT-IR (KBr, cm^{-1}): 3112 (m), 3058 (w), 3002 (w), 2993 (m), 2863 (w), 2826 (w), 1866 (s), 1818 (s), 1748 (s), 1748 (s), 1596 (w), 1542 (m), 1503 (s), 1447 (s), 1404 (m), 1319 (w), 1283 (s), 1226 (w), 1184 (m), 1170 (m), 1134 (w), 1088 (m), 1071 (s), 1031 (w), 986 (m), 934 (w), 897 (s), 759 (s), 721 (s), 701 (s), 645 (w), 626 (w), 556 (w), 509 (w), 468 (w).

dx.doi.org/10.1021/ic501765g | Inorg. Chem. 2014, 53, 12809−12821

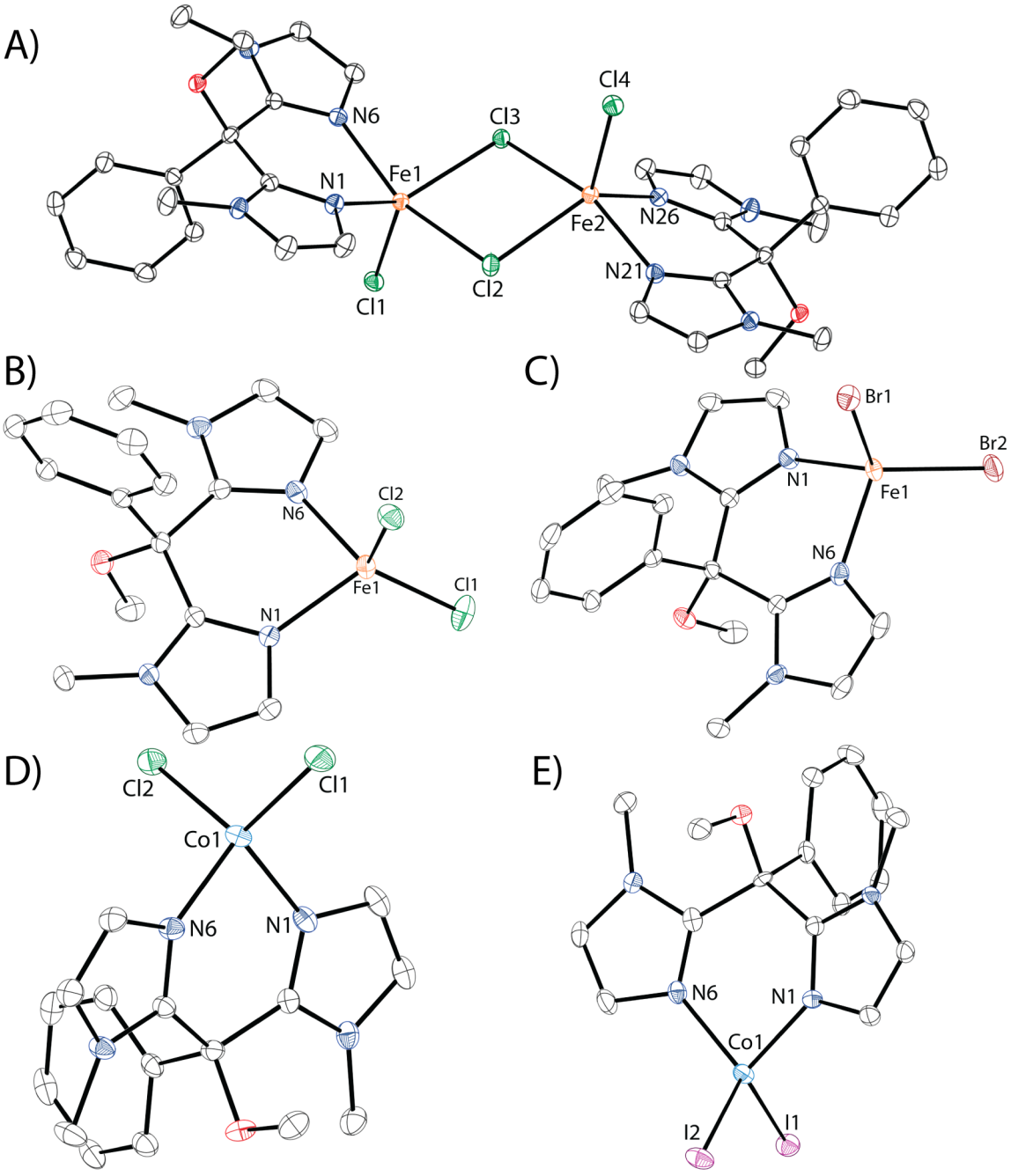

Figure 1. ORTEP representations of the X-ray crystal structures of (A) dimeric **1**, (B) mononuclear **1**, (C) **2**, (D) **3**, and (E) **4**. Thermal ellipsoids are shown at 50% probability. Solvent molecules and hydrogen atoms are omitted for clarity. Color scheme: iron, orange; cobalt, light blue; chlorine, dark green; bromine, dark red; iodine, purple; nitrogen, dark blue; oxygen, red; carbon, colorless.

Synthesis of [Co(BIPhMe)(NO_3)$_2$], 9. In a 20 mL vial, **4** (37.5 mg, 0.0630 mmol) was dissolved in methylene chloride (2 mL). The reaction vessel was capped with a rubber septum, and NO_2(g) was injected until no further color change was observed. The solution turned from emerald green to purple-red. The solution was stirred for 1 h and filtered through glass microfiber filter paper. X-ray-quality crystals of the product were formed upon vapor diffusion of Et_2O over the course of 1 week. The crystals were collected by filtration and washed with Et_2O (3 × 5 mL), resulting in a yield of 6.1 mg (0.0131 mmol, 21%) of **9**. Anal. Calcd for $C_{16}H_{18}CoN_6O_7$: C, 41.30; H, 3.90; N, 18.06. Found: C, 41.19; H, 3.62; N, 17.85. ESI-MS (m/z): 685.4 (calcd $[M + BIPhMe - NO_3]^+$: 685.2). FT-IR (KBr, cm^{-1}): 3128 (m), 3058 (w), 2993 (w), 2932 (m), 2824 (w), 1597 (w), 1500 (s), 1448 (s), 1384 (m), 1315 (s), 1284 (m), 1164 (s), 1089 (m), 1070 (s), 1032 (w), 990 (m), 958 (w), 898 (m), 856 (w), 819 (m), 758 (s), 720 (s), 702 (s), 644 (w), 556 (w), 510 (w).

NO(g)/NO_2(g) Reactions Monitored by UV−Vis Spectroscopy. Solutions of **1**−**4** (102−1120 μM) in MeCN were prepared in the glovebox, removed, and placed in a Cary 50 UV−vis spectrometer. After an initial scan, a syringe of 500 μL gas was injected, and the cuvette was shaken for 10−20 s before being returned to the spectrometer. Scans were collected every 30 s for the first 10 min, every 1 min for the next 20 min, and every 5 min for the final 90 min.

CO(g)/H_2S(g)/O_2(g)/H_2O(l) Reactions Monitored by UV−Vis Spectroscopy. Solutions of **1**−**4** (80−800 μM) in MeCN were prepared in a glovebox, removed, and placed in a Cary 50 UV−vis spectrometer. After an initial scan, a syringe of either 500 μL CO or H_2S gas was injected, an O_2 gas stream was bubbled through the solution, or 100 μL of degassed H_2O was introduced to the cuvette.

dx.doi.org/10.1021/ic501765g | *Inorg. Chem.* 2014, 53, 12809−12821

Table 1. Selected Bond Lengths and Angles of 1−4

compound	M−N (Å)	N−M−N (deg)	M−X (Å)	X−M−X (deg)	N−M−X (deg)
[Fe(BIPhMe)Cl_2], **1**	2.0601(10)	86.53(4)	2.2405(4)	119.778(14)	111.81(3)
	2.0644(10)		2.2638(4)		116.57(3)
					109.91(3)
					107.32(3)
$Fe_2(\mu$-Cl)$_2$(BIPhMe)$_2Cl_2$, **1**·CH_2Cl_2, average values of equivalent atoms	2.1162(11)	83.18(4)	axial:	82.134(11)	89.58(3)
	2.1314(11)		2.2931(4)	98.476(13)	91.20(3)
			bridge:	110.630(15)	99.33(3)
			2.4336(4)		115.70(3)
			2.5025(4)		133.65(3)
					162.06(3)
[Fe(BIPhMe)Br_2], **2**	2.0539(16)	86.75(6)	2.3800(3)	118.618(13)	108.09(4)
	2.0612(16)		2.4058(3)		110.44(4)
					110.55(4)
					117.88(4)
[Co(BIPhMe)Cl_2], **3**	1.9996(10)	91.13(4)	2.2269(4)	114.903(14)	108.32(3)
	1.9961(11)		2.2494(4)		110.51(3)
					112.36(3)
					117.18(3)
[Co(BIPhMe)I_2], **4**	1.990(4)	90.93(15)	2.5510(8)	113.62(3)	106.28(10)
	1.991(4)		2.5594(8)		106.14(11)
					118.48(11)
					120.01(11)

Scans were collected every 60 s for the first 10 min, every 90 s for the next 20 min, and every 4 min for the final 60 min.

Sensor-Loaded Filter Paper NO/NO_2 Test Strips. Strips of filter paper were dipped in separate methylene chloride solutions of **1**−**4** (30−50 mM). Methylene chloride was allowed to evaporate. These integrated filter paper strips were placed in 20 mL vials that were sealed with a septum. NO(g) or NO_2(g) (1 mL) was injected into the vial, and color changes were observed instantly and recorded.

Sensor-Loaded Silica TLC NO/NO_2 Test Strips. Methylene chloride solutions of **1**−**4** (30−50 mM) were spotted on thin-layer chromatography (TLC) plates, and methylene chloride was allowed to evaporate. These TLC plates were placed in a 20 mL vial, and the vial was sealed with a septum. NO(g) or NO_2(g) (1 mL) was injected into the vial, and color changes were observed within 1 min.

Sensor-Loaded Silica Syringe NO/NO_2 Headspace Gas Analyzers. Solutions of **1**−**4** (30−50 mM) in methylene chloride were loaded onto 250−300 mg of silica gel and dried under vacuum. The integrated silica gel was poured into 1 mL plastic syringes fitted with 16 gauge stainless steel needles. NO(g) or NO_2(g) was pulled into the syringe headspace, and color changes were observed instantly.

RESULTS AND DISCUSSION

Synthesis and Spectroscopic Properties of BIPhMe Starting Complexes. The BIPhMe ligand was previously used as a chelating ligand to supply two *cis*-histidine donors in diiron carboxylate complexes.[10] Compounds **1**−**3** are fairly insoluble in THF, whereas their starting materials are soluble. This property allows for easy preparation and purification of the target complexes. Addition of BIPhMe to the metal halide solution afforded rapid precipitation of microcrystalline material. Stirring for an additional 1 h was performed to improve the overall yields. Purification of **1**−**3** was performed by washing with additional THF and Et_2O followed by drying under vacuum. Preparation of pure **4** was not as simple owing to its high solubility in THF, requiring addition of a 1.5 equiv volume of pentanes to precipitate the product. The compound was washed with pentane to remove any residual solvent and subsequently dried under vacuum.

The ^{1}H NMR spectrum of **1** has eight peaks, and the spectrum of **2** has seven. All of these peaks are shifted downfield from those of BIPhMe. The peaks are fairly similar to one another. The differences are that, in the spectrum of **1**, there are peaks at 1.86 and 3.76 ppm, whereas in the spectrum of **2**, there is a single broad peak at 2.83 ppm. This result suggests that the two peaks in **1** may be related and collapse into a single broad peak in **2**. The other difference between the two spectra is that the broad peak at 21.81 ppm and the sharp peak at 18.83 ppm in the spectrum of **1** shift downfield and overlap in the spectrum of **2**.

Complex **1** was observed in a MALDI-TOF-MS experiment using recrystallized anthracene as the matrix. We were also able to observe **1** and **2** losing a halide in the ESI-MS experiment using MeCN as the carrier solvent. During the ESI-MS experiment, we also observed the binding of an additional BIPhMe ligand to iron. Because there was not a second set of peaks in the ^{1}H NMR experiment, it does not appear that an equilibrium exists in solution that involves dissociation and binding of an additional BIPhMe ligand.

In the ^{1}H NMR spectrum of **3**, seven peaks are present, whereas we only observe six peaks in the spectrum of **4**. The BIPhMe peaks are all shifted downfield, as in the iron complexes. The farthest downfield peak for **3** occurs at 37.95 ppm, but this resonance is not observed in the spectrum of **4**. We propose that the peak broadens sufficiently to be observed under these experimental conditions. As in the ESI-MS spectra of the iron-containing compounds, **3** and **4** display peaks corresponding to the complexes minus a halide. These spectra also have peaks that correspond to the binding of an additional BIPhMe ligand to the complex. The ^{1}H NMR spectra of **3** and **4** do not suggest that a (BIPhMe)$_2$ complex exists in solution.

X-ray Crystallographic Characterization of BIPhMe Starting Complexes. Crystallization of compound **1** resulted in two different structures, a mononuclear complex and two chloro-bridged dimers cocrystallized with two half-occupied molecules of methylene chloride (Figure 1). Both crystals were

dx.doi.org/10.1021/ic501765g | Inorg. Chem. 2014, 53, 12809−12821

Table 2. X-ray Crystallographic Data for 1−4 at 100 K

	1	$1_2 \cdot CH_2Cl_2$	2	3	4
formula	$C_{16}H_{18}Cl_2FeN_4O$	$C_{33}H_{38}Cl_6Fe_2N_8O_2$	$C_{16}H_{18}Br_2FeN_4O$	$C_{16}H_{18}Cl_2CoN_4O$	$C_{16}H_{18}CoI_2N_4O$
fw	409.09	903.12	498.01	412.17	595.07
cryst syst	monoclinic	monoclinic	monoclinic	monoclinic	monoclinic
space group	$P2_1/n$	$P2_1/n$	$P2_1/n$	$P2_1/n$	$P2_1/n$
a, Å	10.2648(6)	16.4602(8)	10.4191(3)	10.2460(5)	10.7833(18)
b, Å	14.0109(8)	18.1395(9)	14.3550(3)	13.9051(7)	13.324(2)
c, Å	13.2276(7)	25.8784(13)	13.3245(3)	13.2175(7)	14.141(2)
β, deg	104.5200(10)	93.9280(10)	104.8480(10)	104.3620(10)	100.339(3)
V, Å^3	1841.62(18)	7708.6(7)	1926.35(8)	1824.27(16)	1998.8(6)
Z	4	8	4	4	4
ρ_{calcd}, g/cm^3	1.475	1.556	1.717	1.501	1.977
μ, mm^{-1}	1.119	1.211	4.941	1.244	3.958
θ range, deg	2.15−27.11	1.37−30.79	2.12−26.05	2.16−27.11	2.12−27.19
completeness to θ, %	100.0	99.2	99.9	99.9	99.8
reflns collected	33463	180470	42104	32974	35044
indep reflns	4059	23955	3807	4018	4428
R(int)	0.0282	0.0335	0.0244	0.0290	0.0735
restraints	0	0	0	0	0
param	220	931	220	220	220
max, min transmn	0.7455, 0.6781	0.7461, 0.6556	0.7453, 0.5302	0.7455, 0.6604	0.7455, 0.6137
R1 (wR2) [$I > 2\sigma(I)$]	0.0235 (0.0714)	0.0285 (0.0736)	0.0194 (0.0513)	0.0231 (0.0704)	0.0347 (0.0549)
R1 (wR2)	0.0273 (0.0729)	0.0385 (0.0779)	0.0219 (0.0519)	0.0262 (0.0718)	0.0530 (0.0571)
GoF(F^2)	1.590	1.457	1.760	1.695	1.536
max, min peaks, e/Å^3	0.495, −0.226	0.760, −0.890	0.336, −0.365	0.351, −0.231	1.012, −0.712

grown by vapor diffusion of Et_2O into a methylene chloride solution of the compound at ambient temperature. Crystals of the mononuclear species form as colorless rods, while the dimer complex forms colorless blocks. The mononuclear species contains a pseudotetrahedral iron with a Cl−Fe−Cl angle of 119.778(14)° and Fe−Cl bond distances of 2.2405(4) and 2.2638(4) Å (Table 1).

The chloride-bridged dimer has two pseudo-square-pyramidal iron centers with axial chlorides. The average Cl−Fe−Cl angles are 82.134(11)°, 98.476(13)°, and 110.630(15)°. The average Fe−Cl bond distances are 2.4336(4) and 2.5025(4) Å for the bridging chlorides and 2.2931(4) Å for the axial chloride. The average Fe−Cl−Fe angles are 97.124(13)° and 98.369(13)°. The average N−Fe−N bond angle is more acute in the dimer, 83.18(4)°, compared to the mononuclear complex, 86.53(4)°, resulting in elongation of the Fe−N bond by more than 0.5 Å. Compound **2** also crystallizes as a pseudotetrahedral complex (Figure 1C) with a Br−Fe−Br bond angle of 118.618(13)° and Fe−Br bond distances of 2.3800(3) and 2.4058(3) Å.

Compounds **3** and **4** both crystallize as pseudotetrahedral mononuclear complexes. Compound **3** has a Cl−Co−Cl bond angle of 114.903(14)° and Co−Cl bond distances of 2.2269(4) and 2.2494(4) Å. Compound **4** has a I−Co−I bond angle of 113.62(3)° and Co−I bond distances of 2.5510(8) and 2.5594(8) Å. The N−M−N bond angles of these cobalt complexes are larger by ∼5° compared to those of the iron analogues.

Reactions of Fe^{II}(BIPhMe) Complexes. The reaction of colorless **1** with NO(g) results in the formation of the MNICs $[Fe(BIPhMe)_2(NO)Cl]^+$ and $[Fe(NO)Cl_3]^-$, **5**. The reaction occurs rapidly in methylene chloride, MeCN, and methanol, and a dark-green solution forms. The UV−vis spectrum (Figure 2A) shows absorption bands at 363, 473, and 699 nm. The band at 363 nm is ascribed to $[Fe(NO)Cl_3]^-$ based on the published literature value of 360 nm.[18] The two bands at 473 and 699 nm are assigned to the octahedral

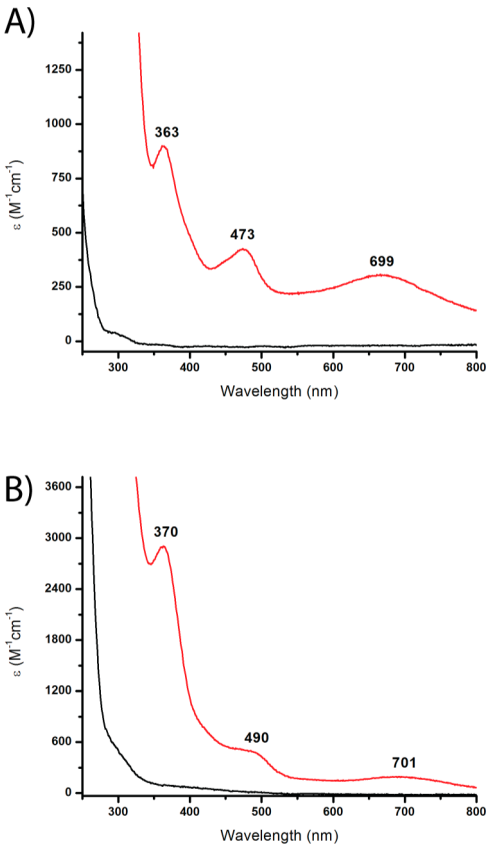

Figure 2. UV−vis spectra of (A) **1** and (B) **2** and their NO(g) products. Color scheme: black, starting material; red, nitrosylated product.

dx.doi.org/10.1021/ic501765g | Inorg. Chem. 2014, 53, 12809−12821

$[Fe(BIPhMe)_2(NO)Cl]^+$ cation. These values are similar to the absorption bands of the published complex $[Fe(TPA)(O_2CCH_3)(NO)]^+$, which are 430 and 650 nm and have extinction coefficients of 730 and 150 M^{-1} cm^{-1}, respectively.[19]

The formation of these bands allows **1** to be used in quantitative and qualitative assays to measure NO(g) release into the headspace of a reaction. A solution of **1** could be prepared and arranged to share the headspace of a reaction that may evolve NO(g) and subsequently convert **1** to **5**. This conversion could be qualitatively observed by the formation of a green solution from a colorless starting solution (Figure 3),

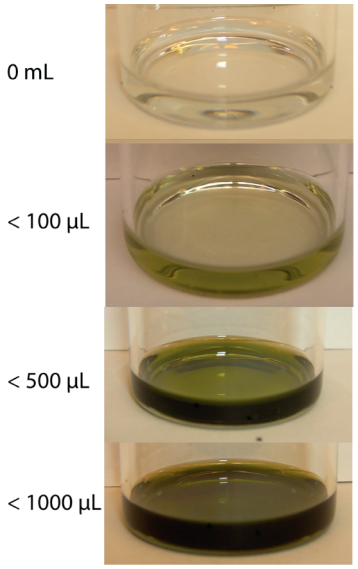

Figure 3. Methylene chloride solution of **1** (24 mM) that was exposed to varying amounts of NO(g).

with less than 2 μmol of NO(g) added. To quantify the conversion, the solution of **1**/**5** could then be transferred to a volumetric flask and appropriately diluted to measure the absorbance. Because **1** does not absorb at 363, 473, or 699 nm, there is no interference with quantification of the formation of **5**.

The IR spectrum of **1** shows two bands at 1709 and 1792 cm^{-1} (Figure 4A) assigned to the ν_{NO} stretching vibration. Upon reaction with ^{15}NO, these bands shift to 1681 and 1757 cm^{-1}, which are close to the values of 1678 and 1760 cm^{-1} computed by the harmonic oscillator model. The ν_{NO} band at 1792 cm^{-1} is assigned to $[Fe(NO)Cl_3]^-$ based on literature published values of 1777, 1794, and 1806 cm^{-1}.[18,20] The ν_{NO} band at 1709 cm^{-1} is attributed to the complex $[Fe(BIPhMe)_2(NO)Cl]^+$ and is comparable to the published ν_{NO} values of 1720 and 1690 cm^{-1} for the related octahedral complexes *cis*-$[Fe(cyclam)(NO)Cl]^+$ and $[Fe(Me_3\text{-}TACN)(N_3)_2(NO)]$, respectively.[21] The positive-mode ESI-MS spectrum of **5** shows peaks that match the isotopic distribution of $[Fe(BIPhMe)_2Cl]^+$ at m/z 655.2. The negative-mode ESI-MS of **5** has two sets of peaks, which correspond to $[FeCl_3]^-$ and $[FeCl_2]^-$ at m/z 162.6 and 125.8, respectively.

The reaction of **2** with NO(g) forms a similar product, **6**. The UV−vis spectrum of **6** shows bands at 370, 490, and 701 nm (Figure 2B). The IR spectrum of **6** (Figure 4B) shows ν_{NO} bands at 1705 and 1791 cm^{-1}. The ESI-MS spectrum shows isotopic patterns for $[Fe(BIPhMe)_2Br]^+$, $[FeBr_3]^-$, and $[FeBr_2]^-$ at m/z 701.1, 296.5, and 252.6, respectively.

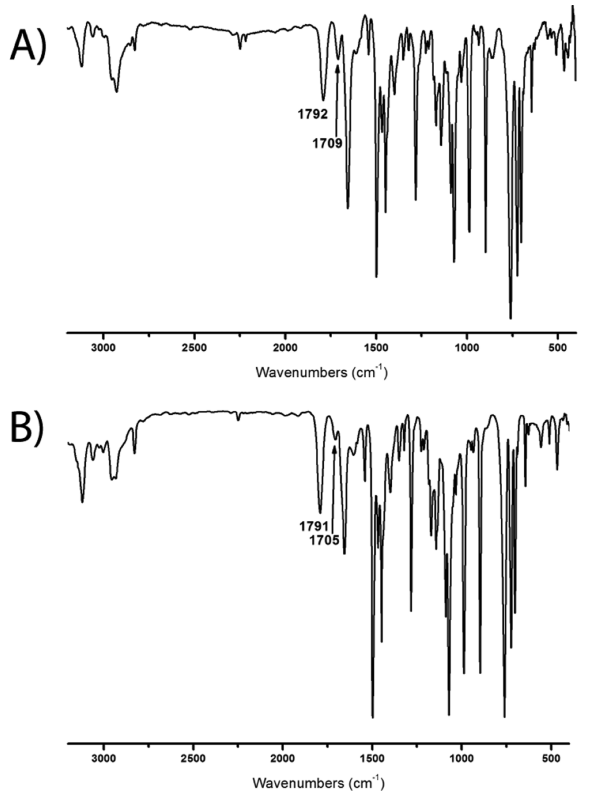

Figure 4. FT-IR spectra of (A) **5** and (B) **6** following reaction with NO.

Crystals of **5** were obtained by vapor diffusion of Et_2O into a methylene chloride solution of the compound over the course of 2 days. The structure contains a bent MNIC, $[Fe(BIPhMe)_2(NO)Cl]^+$, a linear MNIC, $[Fe(NO)Cl_3]^-$, and a disordered methylene chloride solvent molecule (Figure 5A). The Fe−N−O angle of the octahedral complex is 148.9(3)°, and the N−O bond distance is 1.102(3) Å, both of which are lower than the published values for $[Fe(Me_3\text{-}TACN)(N_3)_2(NO)]$ (Table 3). The Fe−N−O angle in the tetrahedral complex is 170.6(3)°, and the N−O bond distance is 1.153(3) Å. These values match those published, 177(1)° and 1.12(2) Å.[22] To verify that the anion was actually $[Fe(NO)Cl_3]^-$ instead of $[FeCl_4]^-$, the NO ligand was replaced with chloride during the structure refinement. This substitution resulted in the thermal ellipsoid of the substituted chloride being elongated along the Fe−Cl bond, showing that the electron density of the appropriate ligand was spread linearly along the bond axis and that a linear NO ligand is the correct assignment. The final structure solution does contain residual electron density trans to the N11 atom at a distance of 1.1 Å from the Fe10 atom. The geometric parameters of the $[Fe(NO)Cl_3]^-$ complex are similar to the published values, confirming that our atom assignment and refinement are true (Table 2).[22] Crystals of **6** were obtained, and refinement of $[Fe(BIPhMe)_2(NO)Br]^+$ proceeded satisfactorily, but the NO moiety is disordered over multiple positions with the Br^- ligands on the $[Fe(NO)Br_3]^-$ complex, resulting in an overall unsatisfactory refinement.

Reaction of **1** with NO_2(g) results in the formation of yellow-orange complex **7** (Figure 6) and presumably N_2O and another iron(III) nitrate species; however, we do not have any experimental data to support this conclusion. The UV−vis spectrum of **7** (Figure 7A) has a shoulder at 335 nm with an

dx.doi.org/10.1021/ic501765g | *Inorg. Chem.* 2014, 53, 12809−12821

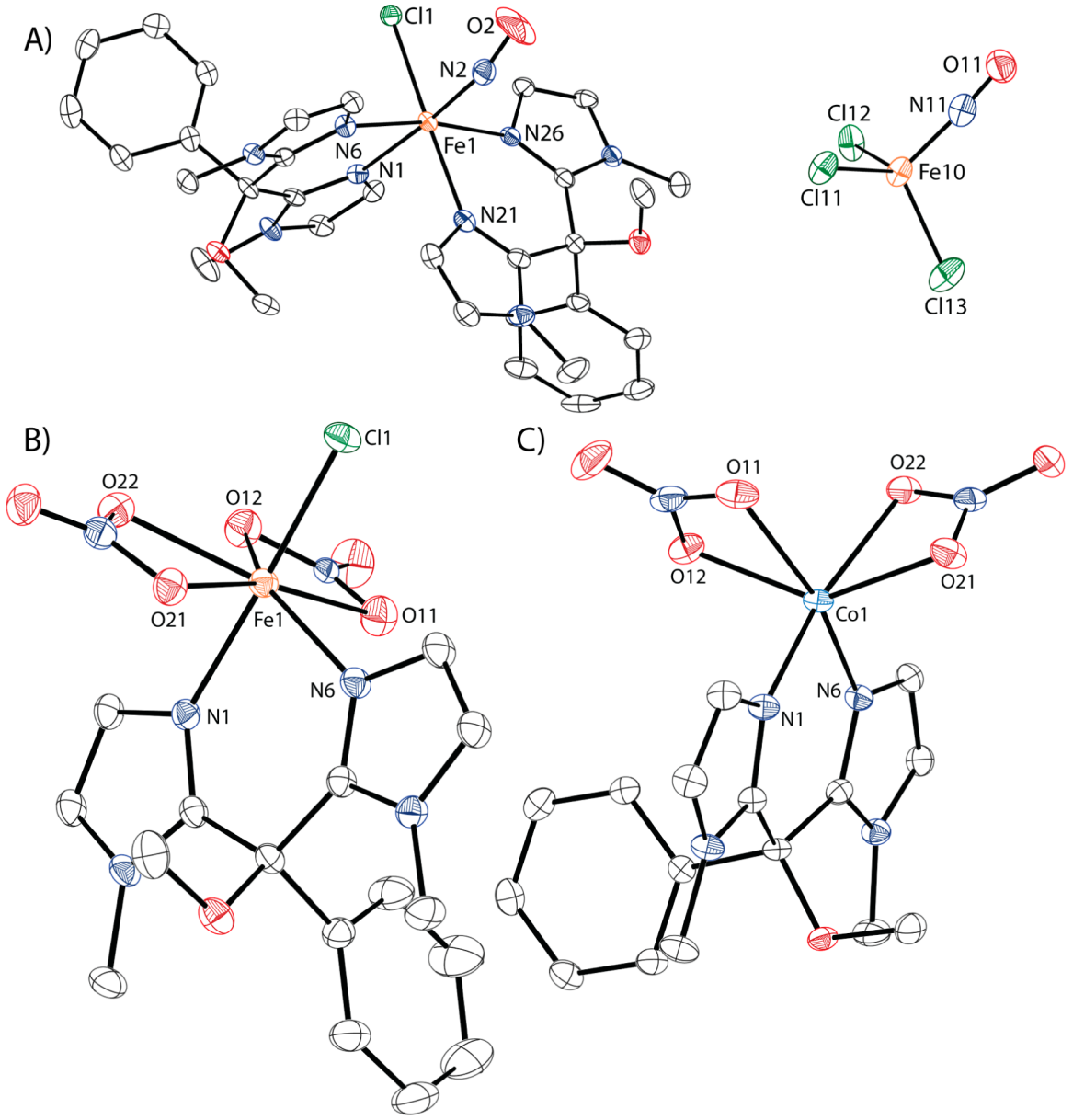

Figure 5. ORTEP representations of the X-ray crystal structures of (A) **5**, (B) **7**, and (C) **9** with thermal ellipsoids shown at 50% probability. Hydrogen atoms and solvent molecules are omitted for clarity. Color scheme: iron, orange; cobalt, light blue; chloride, dark green; nitrogen, blue; oxygen, red; carbon, colorless.

extinction coefficient of 568 $M^{-1}cm^{-1}$. The ESI-MS spectrum shows an isotopic distribution that matches values expected for the complex and an additional bound BIPhMe ligand.

The seven-coordinate iron(III) compound **7** has a pentagonal-bipyramidal geometry with the oxygen atoms of the nitrate ligands and one of the nitrogen atoms of the BIPhMe ligand in the equatorial plane and the other nitrogen atom of the BIPhMe ligand and the chloride atom occupying the apical positions (Figure 5B). The Fe−N bond distances involving the BIPhMe ligand are 2.0819(12) and 2.0882(12) Å, and the N−Fe−N bond angle is 85.84(5)°. The Fe−O bond distances are 2.1357(11), 2.1439(11), 2.1860(11), and 2.1974(12) Å. A B-level alert is generated for this structure in the CheckCIF report based on the Hirshfeld test difference of 10.0 su of atoms O5 and N5, but looking at the plotted thermal ellipsoids at 50% probability, neither atom appears to have motion that would suggest an error (Table 5).

The internal O−Fe−O bond angles involving the nitrate ligands are 59.43(4)° and 59.54(4)°. The interligand O−Fe−O bond angles are 76.26(4)°, 135.56(4)°, 135.69(4)°, and 163.81(4)°. The O−Fe−N_{eq} bond angles are 81.75(5)°, 82.41(5)°, 140.71(5)°, and 141.28(5)°. The O−Fe−N_{ax} bond angles are 86.23(5)°, 86.24(4)°, 87.68(4)°, and 87.84(5)°. The Fe−Cl bond distance is 2.2651(4) Å. The Cl−Fe−N_{ax} bond angle is 178.03(4)°, the Cl−Fe−N_{eq} bond angle is 95.53(3)°, and the Cl−Fe−O bond angles are 91.08(3)°, 91.80(3)°, 93.58(3)°, and 93.75(3)°. The iron atom is not coplanar with the equatorial ligands but rather drawn toward the chloride ion, as indicated by X_{eq}−Fe−Cl angles >90°. According to a search of the Cambridge Structural Database, this compound is the first to have a bidentate nitrogen-binding ligand, two bidentate nitrates, and a non-oxygen ligand. The binding motif is similar to that in other known seven-coordinate iron(III) nitrates with bidentate nitrogen-binding ligands:

dx.doi.org/10.1021/ic501765g | *Inorg. Chem.* 2014, 53, 12809−12821

Table 3. Selected Bond Lengths and Angles and Vibrational Stretches of 5 and Related Compounds

	$[Fe(BIPhMe)_2(NO)Cl]^+$, 5^+	$[Fe(Me_3TACN)(N_3)_2(NO)]$[21a]	$[Fe(NO)Cl_3]^-$, 5^-	$[Fe(NO)Cl_3]^-$ [22]
		Bond Length (Å)		
$Fe-N_{NO}$	1.818(3)	1.738(5)	1.738(3)	1.700(10)
$N_{NO}-O$	1.102(3)	1.142(7)	1.153(3)	1.120(20)
$Fe-X^a$	2.4043(8)	2.075(4)	2.2207(11)	2.224(7)
		2.032(4)	2.2320(9)	2.258(7)
			2.2340(9)	2.228(8)
		Bond Angle (deg)		
$Fe-N_{NO}-O$	148.9(3)	155.5(10)	170.6(3)	177.0(1)
$X-Fe-N_{NO}{}^a$	87.50(9)	97.2(3)	109.93(10)	109.8(5)
		94.2(3)	109.70(10)	111.0(5)
			104.69(10)	103.3(5)
ν_{NO} (cm^{-1})	1709	1690	1792	1802
				1794[20b]
				1777[18]

[a] $X = Cl^-$ or N_3^-.

Table 4. X-ray Crystallographic Data for Compounds $5{\cdot}CH_2Cl_2$, $7{\cdot}0.5CH_2Cl_2$, and 9 at 100 K

	$5{\cdot}CH_2Cl_2$	$7{\cdot}0.5CH_2Cl_2$	9
formula	$C_{33}H_{38}Cl_4Fe_2N_{10}O_4$	$C_{16.5}H_{19}Cl_2FeN_6O_7$	$C_{16}H_{18}CoN_6O_7$
fw	878.21	540.13	465.29
cryst syst	monoclinic	monoclinic	monoclinic
space group	$P2_1/n$	$P2_1/c$	$C2/c$
a, Å	17.7234(6)	9.5411(3)	15.3271(6)
b, Å	12.4526(4)	13.6642(5)	10.6612(4)
c, Å	20.6292(7)	17.0791(6)	24.0172(9)
β, deg	110.4730(10)	93.3630(10)	101.1750(10)°
V, $Å^3$	4265.3(2)	2222.79(13)	3850.1(3)
Z	4	4	8
ρ_{calcd}, g/cm^3	1.368	1.614	1.605
μ, mm^{-1}	0.976	0.970	0.945
θ range, deg	1.31–25.73	1.91–30.94	1.73–30.92
completeness to θ, %	100.0	95.0	94.9
reflns collected	70218	47637	41408
indep reflns	8151	6682	5800
R(int)	0.0620	0.0219	0.0366
restraints	0	0	0
param	476	310	274
max, min transmn	0.7453, 0.6664	0.7461, 0.6563	0.7461, 0.6672
R1 (wR2) [$I > 2\sigma(I)$]	0.0455 (0.1156)	0.0369 (0.1315)	0.0306 (0.0759)
R1 (wR2)	0.0622 (0.1213)	0.0399 (0.1338)	0.0418 (0.0808)
GoF(F^2)	1.232	2.067	1.344
max, min peaks, $e/Å^3$	2.518, −0.654	1.048, −1.198	0.468, −0.236

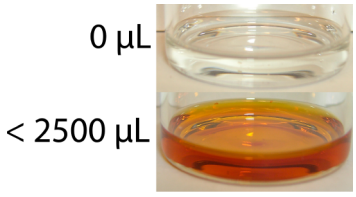

Figure 6. Methylene chloride solution of **1** that was exposed to excess NO_2(g).

{*cis*-$[Ru(CN\text{-}^tBu)_4(CN)_2]Fe(NO_3)_3\}_2$, $[Fe_2(\mu\text{-}O)(bpy)_2(NO_3)_4]$, and $[Fe_2(\mu\text{-}O)L)(NO_3)_4]$, where L is an ethylene-bridged bis(bpy) ligand.[23] Seven-coordinate iron(III) complexes are relatively rare, comprising only 0.7% of the published iron-containing crystal structures in the Cambridge Structural Database.[24]

Similar to the formation of **7**, compound **8** forms from the reaction of **2** and NO_2(g). This reaction can be followed using UV–vis spectroscopic changes involving the formation of bands at 290 and 360 nm (Figure 7B). The visible absorption bands of **8** are more intense than the bands observed for **7**.

The reactivity of **1** and **2** with other potential small molecules was tested by observing changes in the UV–vis spectrum of the complexes upon introduction of the reactant. As expected, complexes **1** and **2** were determined to be sensitive to O_2(g) but did not display any significant spectral changes upon introduction of CO(g), H_2S(g), or H_2O(l) (Supporting Information, Figures S19–S26).

Reactions of 3 and 4 with NO(g) and NO_2(g). Compound **3** does not react with NO(g), judging by UV–vis or IR spectroscopy. Reaction of **4** in methylene chloride with NO(g) results in a color change from deep green to dark

dx.doi.org/10.1021/ic501765g | Inorg. Chem. 2014, 53, 12809–12821

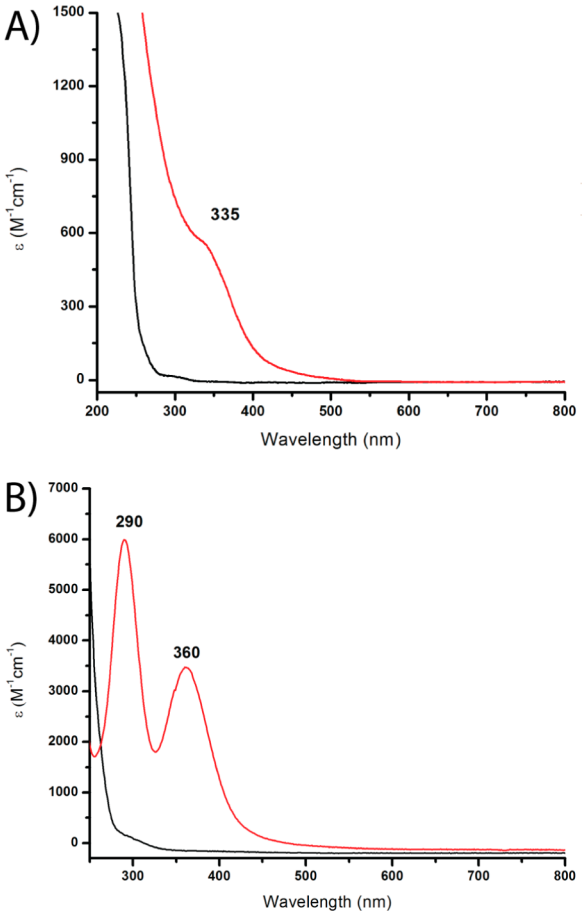

Figure 7. UV−vis spectra of (A) **1** and (B) **2** and their NO_2(g) products. Color scheme: black, starting material; red, reaction product.

yellow. When this reaction is followed by UV−vis spectroscopy (Figure 8A/B), the bands at 244 nm and from 583 to 668 nm are diminished upon addition of excess NO(g). The bands at 310 and 373 nm blue shift and increase in intensity to 293 and 362 nm. These two new, high-energy bands may be associated with the I_3^- ion, which has absorption maxima at 297 and 350 nm.[26] Cobalt-mediated iodide oxidation may be the reaction route observed, resulting in the formation of a new species that cannot be identified by optical spectroscopy from the crude product.

The positive-mode ESI-MS spectrum (Figure 9) of the crude product shows two sets of peaks, with the most abundant ions located at m/z 341.1 and 371.1. These two peaks correspond well with the potential ions of $[Co(BIPhMe)(NO)]^+$, calculated to have a mass of m/z 371.1, and $[Co(BIPhMe)]^+$, calculated to have a mass of m/z 341.1. Both of these ions may form from the synthetically possible $[Co(BIPhMe)(NO)_2]^+$ complex. Evidence for the formation of complex $[Co(BIPhMe)_2(NO)_2]^+$ is observed in the ESI-MS spectrum by the group of peaks with the most abundant ion located at m/z 668.2, which matches well with the calculated value of m/z 668.2 for the parent ion minus a methyl group, and the presence of a group of peaks that matches $[Co(BIPhMe)_2(NO)]^+$. The negative-mode ESI-MS shows peaks at m/z 312.6 ($[CoI_2]^-$, calcd m/z 312.7), 380.5 (I_3^-, calcd m/z 380.7), and 439.5 ($[CoI_3]^-$, calcd m/z 439.6).

The FT-IR spectrum of the crude nitrosylated product of **4** shows bands at 1748, 1784, 1818, and 1866 cm^{-1} (Figure 8C). The shape and separation of the bands suggest the formation of two distinct cobalt dinitrosyl species. One of these putative cobalt dinitrosyl species would consist of bands at 1748 and 1818 cm^{-1}, which we could assign as either $[Co(NO)_2(I_3)]^-$ (1758 and 1820 cm^{-1}) or $[Co(NO)_2(I_2)]^-$ (1738 and 1820

Table 5. Selected Bond Lengths and Angles of 7, 9, and Related Compounds

	7		$[Fe(bpy)(NO_3)_2]_2O$[23c]		9		$Co(^{Ph,Ph}Me\text{-}Im)_2(NO_3)_2$[25]	
				Bond Length (Å)				
M−N	axial:	equatorial:	axial:	equatorial:	2.0242(11)		2.024(1)	
	2.0819(12)	2.0882(12)	2.178(2)	2.141(2)	2.0330(11)		2.024(1)	
M−O	2.1357(11)		2.159(2)		2.2136(10)		1.996(1)	
	2.1439(11)		2.263(2)		2.0903(10)		2.709(1)	
	2.1439(11)		2.143(2)		2.0766(10)		2.014(1)	
	2.1974(12)		2.204(2)		2.2398(10)		2.446(1)	
M−Cl/O_{bridge}	2.2651(4)		1.7761					
				Bond Angle (deg)				
O−M−O	intra:	inter:	intra:	inter:	intra:	inter:	intra:	inter:
	59.43(4)	76.26(4)	57.97(7)	75.07(7)	59.94(4)	91.71(4)	56.47(4)	81.99(5)
	59.54(4)	135.56(4)	59.02(8)	134.00(8)	59.80(4)	94.04(4)	51.69(4)	83.55(5)
		135.69(4)		132.82(8)		94.50(4)		105.22(5)
		163.81(4)		166.32(8)		141.08(4)		108.04(5)
N−M−N	85.84(5)		75.03(8)		90.95(4)		97.6(1)	
N−M−O	axial:	equatorial:	axial:	equatorial:	89.34(4)	96.32(4)	126.08(5)	100.08(5)
	86.23(5)	82.41(5)	87.75(8)	136.29(8)	110.43(4)	169.53(4)	91.81(5)	137.24(5)
	86.24(4)	81.75(5)	82.45(8)	79.82(8)	164.18(4)	102.99(4)	89.61(5)	148.79(5)
	87.68(4)	140.71(5)	92.04(8)	143.71(8)	104.33(4)	88.00(4)	91.81(5)	90.15(5)
	87.84(5)	141.28(5)	90.86(8)	86.93(8)				
N−M−Cl/O_{bridge}	178.03(4)	95.53(3)	169.20	95.31				
O−M−Cl/O_{bridge}	93.58(3)	96.32						
	91.80(3)	91.20						
	91.08(3)	98.68						
	93.75(3)	93.45						

dx.doi.org/10.1021/ic501765g | Inorg. Chem. 2014, 53, 12809−12821

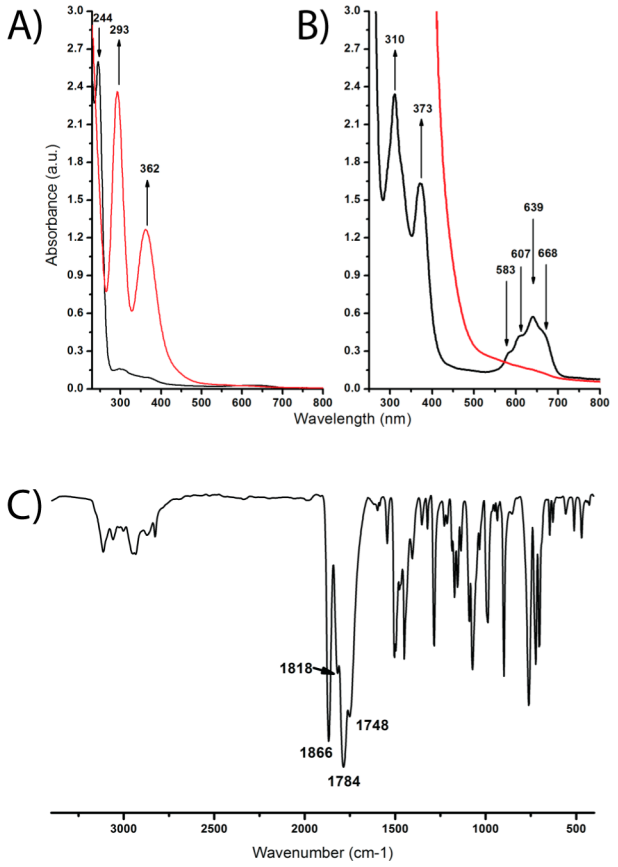

Figure 8. Spectroscopic characterization of the product generated by reaction of **4** and NO(g). The UV−vis spectrum (A and B) was recorded in MeCN (1.02 mM) under nitrogen. The FT-IR spectra (C) was recorded as a KBr pellet.

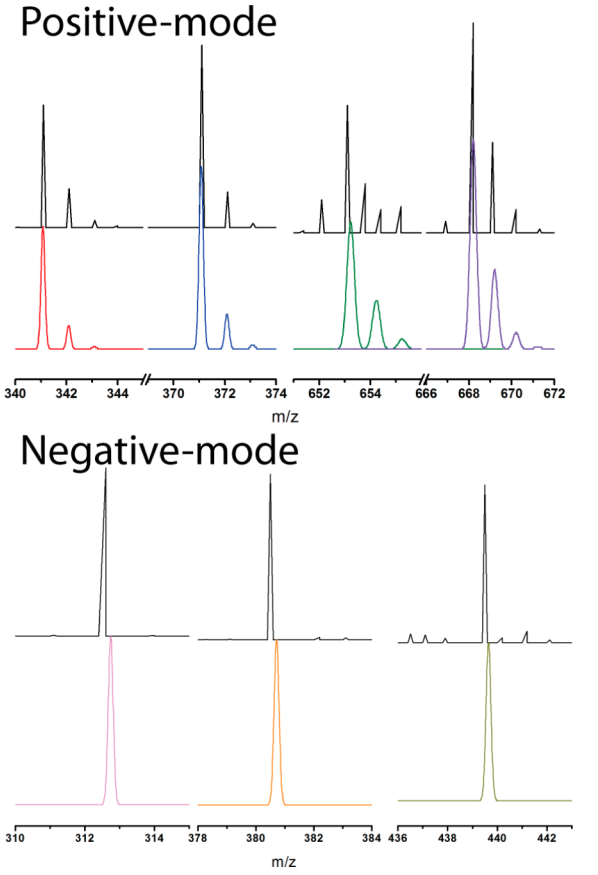

Figure 9. Positive-mode (top) and negative-mode (bottom) ESI-MS spectra of the product formed in the reaction of **4** and NO(g) in MeCN. Color scheme: experimental, black; simulated $[Co(BIPhMe)]^+$, red; simulated $[Co(BIPhMe)(NO)]^+$, blue; simulated $[Co(BIPhMe)_2(NO)]^+$, green; simulated $[Co(BIPhMe)_2(NO)_2CH_3]^+$, violet; simulated $[CoI_2]^-$, pink; simulated $[I_3]^-$, orange; $[CoI_3]^-$, dark yellow.

cm^{-1}), based on literature values and the observed mass spectrum.[27] The other cobalt dinitrosyl species would have bands at 1784 and 1866 cm^{-1}, which could be either the $[Co(BIPhMe)(NO)_2]^+$ or $[Co(BIPhMe)_2(NO)_2]^+$ species observed in the mass spectrum. Attempts at crystallization, separation, and structural characterization of the two nitrosyl species proved to be unsuccessful.

Reaction of **3** with NO_2(g) in methylene chloride results in a color change from deep blue to dark green. This color change can be followed by UV−vis spectroscopy (Figure 10A) by the growth of new bands at 359 and 700 nm. A decrease in intensity of the bands at 554 and 632 nm is also observed, suggesting that the chloride ligands are retained. This conclusion is further corroborated by the presence of $[Co(BIPhMe)_2(NO_3)]^+$ and $[Co(BIPhMe)_2Cl]^+$ ions in the ESI-MS spectrum.

Exposure of **4** to NO_2(g) in methylene chloride results in a color change from dark green to red-purple, from which the pink complex **9** could be isolated. This qualitative color change corresponds to loss of the absorption band at 244 nm and the cluster of bands ranging from 583 to 668 nm (Figure 10C). A new, broad band grows in at 462 nm along with a shoulder at 270 nm (Figure 10B). These two spectral features correspond well with the formation of I_2, which has absorption bands at 288, 350, and 460 nm.[26] The absorption band at 350 nm is obscured by the absorption bands of dissolved NO_2(g).

Compound **9** crystallizes in space group *C*2/*c* with a six-coordinate cobalt(II) center (Figure 5C). The compound has Co−N bond distances of 2.0242(11) and 2.0330(11) Å and a 90.95(4)° N−Co−N bond angle. Both nitrates are bidentate and bound to the cobalt by the oxygen atoms. The Co−O bond distances are 2.0766(10), 2.0903(10), 2.2136(10), and 2.2398(10) Å. The inter O−Co−O bond angles are 59.94(4) and 59.80(4)°, and the intra O−Co−O bond angles are 91.71(4), 94.04(4), 94.50(4), and 141.08(4)°. The O−Co−N bond angles are 88.00(4), 89.34(4), 96.32(4), 102.99(4), 104.33(4), 110.43(4), 164.18(4), and 169.53(4)°. The ligands form a propeller-like geometry around the cobalt due to the acute O−Co−O angles.

No spectral changes were observed in the UV−vis spectrum upon addition of O_2(g), CO(g), or H_2S(g) to solutions of **3** or **4** in MeCN. Addition of H_2O(l) resulted in loss of band intensity for both species (Supporting Information, Figures S27−S34).

Preparation of NO(g)/NO_2(g) Test Strips and Syringes. Experimentalists desire rapid and facile methods to detect chemical changes. Colorimetric test strips are commonly used in synthetic chemistry and biology to quickly evaluate pH changes in aqueous solutions or quantitatively observe H_2S release, using $Pb(OAc)_2$ strips, and metals ions, such as Al^{3+}, Co^{2+}, and Cu^{2+}. These strips are available commercially from scientific vendors.[28]

dx.doi.org/10.1021/ic501765g | *Inorg. Chem.* 2014, 53, 12809−12821

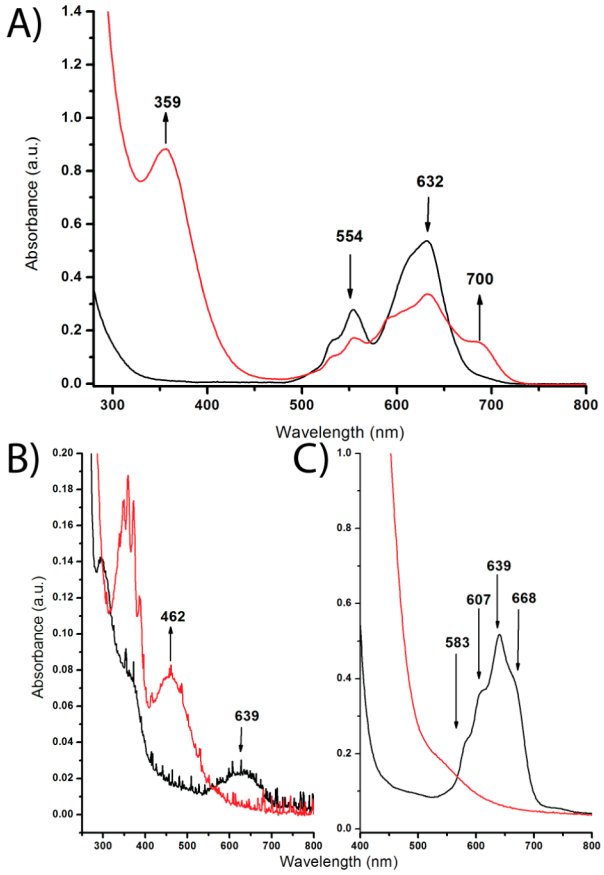

Figure 10. Spectroscopic characterization of the product generated by the reaction of **3** (A) and **4** (B and C) with $NO_2(g)$. The UV−vis spectrum was recorded in MeCN (1.12 mM) under nitrogen. Color scheme: black, starting material; red, product.

Compounds **1**−**4** can be loaded onto filter paper from methylene chloride solutions. Exposure to NO(g) or $NO_2(g)$ of these loaded paper strips results in qualitative color changes. This method provides a rapid, low-cost method to qualitatively measure NO(g) or $NO_2(g)$ release from a chemical or biochemical reaction.

These individual strips can be combined into a single test strip by spotting silica TLC plates with multiple solutions of the compounds (Figure 11). These silica-based test strips require less space and allow for direct comparison of gas release from multiple compounds to determine whether the color change profile matches what is expected. Deviations from the color change profile would occur in environments contaminated with gaseous O_2 or H_2O but would still provide information regarding NO(g) or $NO_2(g)$ gas release. Because the cobalt species are insensitive to $O_2(g)$ and the iron ones are insensitive to H_2O, these test strips would still be useful for their colorimetric readout, which could be correlated with a color change in the absence of interfering species. Silica TLC plates have been previously developed as test strips by loading with a colorimetric sensor to detect hypochlorite.[29]

The compounds can be loaded onto silica by dissolving them in methylene chloride and evaporating the solution onto silica gel. This silica gel bound sensor can be loaded into syringes equipped with needles (Figure 12). By pulling the headspace of a reaction through the syringe, the compound will change color and report the formation of NO(g) or $NO_2(g)$ released into the reaction headspace. An added benefit of using this device is

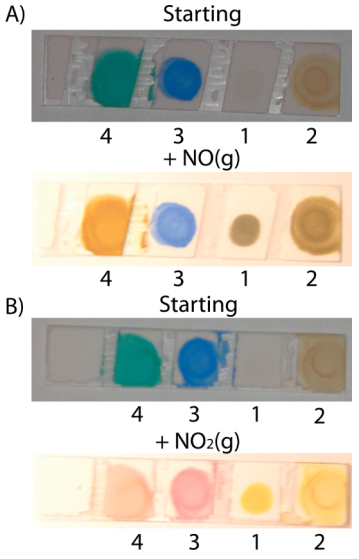

Figure 11. Silica TLC plates loaded with **1**−**4** and exposed to (A) NO(g) and (B) $NO_2(g)$.

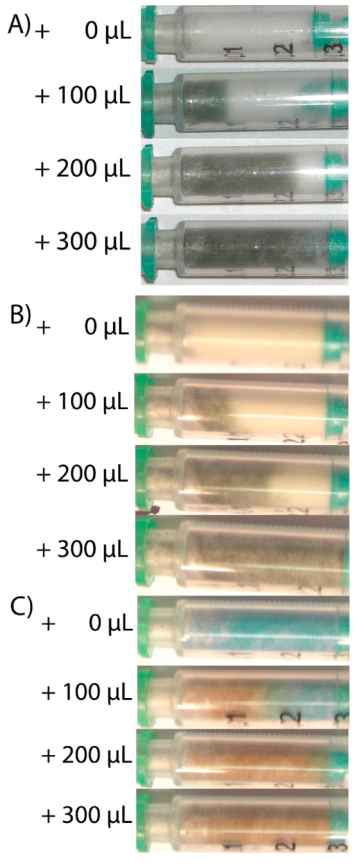

Figure 12. Syringes filled with (A) **1**, (B) **2**, and (C) **4** loaded onto silica gel and exposed to varying amounts of NO(g).

that, by controlling the amount of compound loaded onto the syringe, we can quantitatively measure the amount of gas released in the reaction by how far along the syringe the color change occurs due to the reaction with colorimetric sensors. This rapid quantification can serve as an initial experiment for biochemical studies to determine how much **1** is necessary to more accurately measure the amount of gas released by spectroscopic methods.

dx.doi.org/10.1021/ic501765g | *Inorg. Chem.* 2014, 53, 12809−12821

CONCLUSIONS

New Fe^{2+} and Co^{2+} complexes using the dinitrogen donor ligand BIPhMe were prepared. These complexes were crystallographically and spectroscopically characterized. The iron and cobalt complexes have the general formula $[M(BIPhMe)X_2]$, where M is Fe^{2+} or Co^{2+} and X is Cl^-, Br^-, or I^-.

Reaction of colorless **1** with NO(g) forms the dark-green complex **5**, whereas reaction with NO_2(g) forms the yellow complex **7**. This complex can serve in a quantitative and qualitative assay to measure the release of NO(g) or NO_2(g) from solutions. The yellow compound **2** can be used in a similar manner because it generates structurally similar products but with different spectroscopic properties.

Compound **3** shows no reactivity toward NO(g), but the related compound **4** does react to form two dinitrosyl species, which we assign as a BIPhMe-ligated cation and an iodine-ligated anion. Both Co^{2+} complexes react with NO_2(g) and provide a qualitative change in color.

By using these metal complexes, NO(g) and NO_2(g) test strips were prepared using filter paper or silica TLC plates. These test strips could be placed in enclosed containers that share the headspace with reactions that form NO(g) and NO_2(g) and provide qualitative proof that these gases are generated. To more quantitatively measure gas generation, silica-loaded syringes were used to measure gas amounts.

ASSOCIATED CONTENT

Supporting Information

^{1}H NMR spectra of **1**−**4**, qualitative colorimetric responses of methylene chloride solutions of **1**−**4** to NO(g) and NO_2(g), IR and ESI-MS spectra of **1**−**8**, full depictions of the asymmetric units of the crystal structures, UV−vis spectra upon the addition of other small molecules, and CIF files. This material is available free of charge via the Internet at http://pubs.acs.org.

AUTHOR INFORMATION

Corresponding Author

*E-mail: lippard@mit.edu. Phone: (617) 253-1892. Fax: (617) 258-8150.

Notes

The authors declare no competing financial interest.

ACKNOWLEDGMENTS

This work was supported by Grant CHE1265770 from the National Science Foundation.

REFERENCES

(1) (a) Koshland, D., Jr. *Science* **1992**, *258*, 1861. (b) Furchgott, R. F. *Angew. Chem., Int. Ed.* **1999**, *38*, 1870. (c) Ignarro, L. J. *Angew. Chem., Int. Ed.* **1999**, *38*, 1882. (d) Murad, F. *Angew. Chem., Int. Ed.* **1999**, *38*, 1856.

(2) (a) Bronte, V.; Zanovello, P. *Nat. Rev. Immunol.* **2005**, *5*, 641. (b) Calabrese, V.; Mancuso, C.; Calvani, M.; Rizzarelli, E.; Butterfield, D. A.; Stella, A. M. *Nat. Rev. Neurosci.* **2007**, *8*, 766. (c) Tonzetich, Z. J.; McQuade, L. E.; Lippard, S. J. *Inorg. Chem.* **2010**, *49*, 6338. (d) Szaciłowski, K.; Chmura, A.; Stasicka, Z. *Coord. Chem. Rev.* **2005**, *249*, 2408.

(3) Hetrick, E. M.; Schoenfisch, M. H. *Annu. Rev. Anal. Chem.* **2009**, *2*, 409.

(4) Bates, J. N. *Neuroprotocols* **1992**, *1*, 141.

(5) Davies, I. R.; Zhang, X. Nitric Oxide Selective Electrodes. In *Methods in Enzymology*; Robert, K. P., Ed.; Academic Press: New York, 2008; Vol. *436*, p 63.

(6) (a) Skodje, K. M.; Kwon, M.-Y.; Chung, S. W.; Kim, E. *Chem. Sci.* **2014**, *5*, 2374. (b) Wennmalm, Å.; Lanne, B.; Petersson, A.-S. *Anal. Biochem.* **1990**, *187*, 359.

(7) (a) Abcam. *Nitric Oxide Assay Kit (Colorimetric)*, http://www.abcam.com/ps/products/65/ab65328/documents/ab65328%20Nitric%20Oxide%20Assay%20Kit%20Colorimetric%20.(accessed November 12, 2014). (b) Green, L. C.; Wagner, D. A.; Glogowski, J.; Skipper, P. L.; Wishnok, J. S.; Tannenbaum, S. R. *Anal. Biochem.* **1982**, *126*, 131.

(8) (a) Dacres, H.; Narayanaswamy, R. *Sens. Actuators, B* **2005**, *107*, 14. (b) Meng, Q. T.; Zhang, Y. X.; Hou, D. Y.; Xin, G.; Li, T. C.; He, C.; Duan, C. Y. *Tetrahedron* **2013**, *69*, 636. (c) Rathore, R.; Abdelwahed, S. H.; Guzei, I. A. *J. Am. Chem. Soc.* **2004**, *126*, 13582.

(9) (a) Lim, M. H.; Xu, D.; Lippard, S. J. *Nat. Chem. Biol.* **2006**, *2*, 375. (b) McQuade, L. E.; Pluth, M. D.; Lippard, S. J. *Inorg. Chem.* **2010**, *49*, 8025.

(10) Tolman, W. B.; Liu, S. C.; Bentsen, J. G.; Lippard, S. J. *J. Am. Chem. Soc.* **1991**, *113*, 152.

(11) Lorković, I. M.; Ford, P. C. *Inorg. Chem.* **2000**, *39*, 632.

(12) Pangborn, A. B.; Giardello, M. A.; Grubbs, R. H.; Rosen, R. K.; Timmers, F. J. *Organometallics* **1996**, *15*, 1518.

(13) Kent, T. A. *WMOSS v. 2.5: Mössbauer Spectral Analysis Software*; WEB Research Co.: Minneapolis, MN, 1998.

(14) *APEX2v2009*; Bruker AXS: Madison, WI, 2009.

(15) Sheldrick, G. M. *SADABS: Area-Detector Absorption Correction*; University of Göttingen: Göttingen, Germany, 2008.

(16) (a) Sheldrick, G. *Acta Crystallogr., Sect. A: Found. Crystallogr.* **2008**, *64*, 112. (b) Sheldrick, G. M. *SHELXTL97: Program for Refinement of Crystal Structures*, University of Göttingen: Göttingen, Germany, 1997.

(17) Dolomanov, O. V.; Bourhis, L. J.; Gildea, R. J.; Howard, J. A. K.; Puschmann, H. *J. Appl. Crystallogr.* **2009**, *42*, 339.

(18) Tran, C. T.; Kim, E. *Inorg. Chem.* **2012**, *51*, 10086.

(19) Zang, Y.; Que, L., Jr. *Inorg. Chem.* **1995**, *34*, 1030.

(20) (a) Connelly, N. G.; Gardner, C. *J. Chem. Soc., Dalton Trans.* **1976**, 1525. (b) Kalyvas, H.; Coucouvanis, D. *Polyhedron* **2007**, *26*, 4765.

(21) (a) Pohl, K.; Wieghardt, K.; Nuber, B.; Weiss, J. *J. Chem. Soc., Dalton Trans.* **1987**, 187. (b) Siri, O.; Tabard, A.; Pullumbi, P.; Guilard, R. *Inorg. Chim. Acta* **2003**, *350*, 633.

(22) Steimann, M.; Nagel, U.; Grenz, R.; Beck, W. *J. Organomet. Chem.* **1983**, *247*, 171.

(23) (a) Halbauer, K.; Spielberg, E. T.; Sterzik, A.; Plass, W.; Imhof, W. *Inorg. Chim. Acta* **2010**, *363*, 1013. (b) Seddon, E. J.; Yoo, J.; Folting, K.; Huffman, J. C.; Hendrickson, D. N.; Christou, G. *J. Chem. Soc., Dalton Trans.* **2000**, 3640. (c) Taft, K. L.; Masschelein, A.; Liu, S.; Lippard, S. J.; Garfinkel-Shweky, D.; Bino, A. *Inorg. Chim. Acta* **1992**, *198*−*200*, 627.

(24) Craig, G. A.; Barrios, L. A.; Costa, J. S.; Roubeau, O.; Ruiz, E.; Teat, S. J.; Wilson, C. C.; Thomas, L.; Aromi, G. *Dalton Trans.* **2010**, *39*, 4874.

(25) Kounavi, K. A.; Papatriantafyllopoulou, C.; Tasiopoulos, A. J.; Perlepes, S. P.; Nastopoulos, V. *Polyhedron* **2009**, *28*, 3349.

(26) Li, N.; Shi, L.; Wang, X.; Guo, F.; Yan, C. *Int. J. Anal. Chem.* **2011**, *2011*.

(27) Sacco, A.; Rossi, M.; Nobile, C. F. *Ann. Chim. (Rome)* **1967**, *57*, 499.

(28) Machery-Nagel QUANTOFIX® test strips, http://www.mn-net.com/tabid/4928/default.aspx (accessed April 7, 2014).

(29) Goswami, S.; Paul, S.; Manna, A. *Dalton Trans.* **2013**, *42*, 10097.